Effect of residual gaseous impurities on the dewetting of antimonide melts in fused silica crucibles in the case of bulk crystal growth

Lamine Sylla, Jean Pierre Paulin, Gina Vian, Christian Garnier, Thierry Duffar

Effect of residual gaseous impurities on the dewetting of antimonide melts in fused silica crucibles in the case of bulk crystal growth

L. Sylla *, J.P. Paulin, G. Vian, C. Garnier, T. Duffar

SIMAP-EPM, ENSEEG, BP 75, 38402 Saint Martin d'H`eres, France

A Bridgman set-up has been modified to perform the contactless growth ("dewetting") of gallium and indium antimonide compounds in fused silica crucibles. According to wetting parameters measured by the sessile drop method given in the literature, both molten InSb and GaSb compounds are considered as non-reactive with silica substrates. A detailed description of the experimental set-up is presented. Each polycrystalline sample i s inserted in a sealed silica crucible that is backfilled with industrial argon containing a few ppm of oxygen. Under similar experimental conditions, the dewetted growth of GaSb is much easier to obtain than that for InSb. The presence of residual impurities such as oxygen in the backfilling gas appears to enhance the occurrence of the phenomenon for GaSb.

Keywords: Contact angle; Crystal growth from melt; Dewetted Bridgman technique; III–V semiconducting materials

1. Introduction

The Vertical Bridgman solidification method is used for semiconductor growth. In our experimental configuration, bulk crystals are grown inside a sealed fused silica crucible that is filled with a gas and contains the melted feed material above its solid seed. The system contains therefore three phases: condensed (liquid and solid) and gaseous (backfilling gas and gas compounds formed at equilibrium).

We focus on one phenomenon called "dewetting" [1] or "detachment" [2] by which the solid crystal grows without contact with the crucible wall thanks to the stability of a liquid meniscus joining the two triple-lines (Fig. 1). A direct consequence of this phenomenon is the dramatic improvement of crystal quality (defect density is highly reduced in the dewetted zones of the crystal) and electronic properties. This phenomenon was observed first in microgravity. A review of past microgravity experiments was made by Wilcox and Regel [3]. The occurrence of dewetting mainly depends on the melt/crucible interactions through some critical parameters such as the contact angle θ between the melt and the crucible walls, the growth angle α and the growth atmosphere according to Duffar et al.'s theoretical explanation [1]. The growth angle α corresponds to the contact angle of a melt on its own solid. A theoretical model has been developed to explain the dewetted growth in the case of rough crucibles where the roughness is modelled by sharp or rounded peaks for terrestrial and microgravity conditions [4]. As soon as composite wetting conditions are satisfied, dewetting takes place and the solidification trajectory corresponds to the equation of an infinite spiral. There is a good agreement between experimental and predicted results. Under terrestrial conditions and in the case of a smooth crucible such as silica, the sum of the growth and wetting angles should be high and close to 180°. Nevertheless such a condition is not satisfied for most of the molten semiconductors on practical crucible materials. An additional furnace is used to increase the gas pressure in the gap (Fig. 1) to counterbalance the hydrostatic pressure [5]. The gas pressure difference can be controlled either by manipulating the thermal field or by using accurate external pressure controller [6,7]. It has been observed that the process is self-controlled when the pressure is slightly higher in the gap than the sum of the top gas and hydrostatic pressures ($P_{\mathrm{COLD}} \geq P_{\mathrm{HOT}} + \rho g h$). A single crystal of GaSb has been obtained by this method [5]. However, the range of gas pressure difference values across the meniscus to reach stable dewetted growth is narrow when $\theta + \alpha < 180^{\circ}$ [6,7]. Then an artificial increase of the wetting angle value would be a possible explanation. A number of scientists have put forth the idea of oxidation involvement in dewetting enhancement due

* Corresponding author. Tel.: +33 4 7682 5259; fax: +33 4 7682 5259.
E-mail address: lamine.sylla@gmail.com (L. Sylla).

Table 1
Values of wetting parameters on silica for indium and gallium antimonide [10]

Material	Contact angle θ_Y on SiO_2	Growth angle, α	Surface tension, σ (J m^{-2})	Work of adhesion, W (J m^{-2})	$W/2\sigma$ (%)
InSb	112°	20–30°	0.406	0.271	31
GaSb	121°	10–18°	0.452	0.219	24

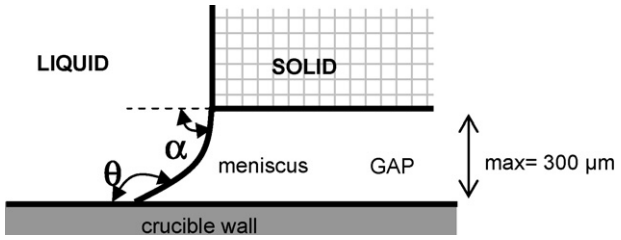

Fig. 1. Enlarged cross-sectional view of the meniscus zone within the crucible.

to molten semiconductor pollution by residual gases or other sources (sample or/and crucible) [8,9].

Most of the successful terrestrial experiments were carried out by using molten semiconductors on non-wetting crucibles materials. Dewetting is predicted to be favoured by high contact angle values of the melt on the crucible walls and high growth angle. Harter et al. [10] performed measurements of GaSb and InSb contact angles on C, BN, AlN, Al_20_3 and SiO_2 substrates by the sessile drop method. The values of contact angles, surface tension, work of adhesion and cohesion on silica are given in Table 1 and on other substrates in Table 2 for both molten compounds. It has been concluded from their work that both antimonides are classified as non-reactive melts with silica and their wetting behaviour depends mainly on the chemical interaction at the melt/substrate interface.

A recent work on the influence of oxygen, hydrogen, helium, argon and vacuum on molten InSb drop has been published by Regel et al. [11] who performed sessile drop experiments with molten InSb on clean fused silica surfaces. The surface tension σ of oxide-free molten InSb was smaller in flowing Ar than in He, seemed to increase with increasing O_2 in the gas, and was not influenced by 10% H_2 or 0.1% Ga in the melt. The contact angle θ on silica was higher in flowing Ar than in He, was lowered by O_2, and was not influenced by H_2 or Ga. The authors concluded that crystal growth should be carried out with a low adhesion work material for the crucible, a reducing agent in the crucible to avoid oxide formation and in the growth atmosphere before sealing. The common choice is to seal the silica crucible in Ar containing H_2 gas with carbon coating on crucible wall as a reducing agent or boron nitride BN owning the lowest adhesion work.

Table 2
Values of wetting parameters on other substrates [10]

	InSb[a]			GaSb[a]		
Substrate	θ	W (J m^{-2})	$W/2\sigma$ (%)	θ	W (J m^{-2})	$W/2\sigma$ (%)
AlN				104°	0.344	38
Al_2O_3	111°	0.278	32	112°	0.283	31
SiO_2	112°	0.271	31	121°	0.219	24
C	124°	0.191	22	128°	0.174	19
BN	134°	0.132	15	132°	0.149	16

[a] Material.

As an illustration, gallium-doped germanium, Ge:Ga, and silicon rich germanium, $Ge_{1-x}Si_x$, have been grown dewetted with resistively heated and monoellipsoid mirror Bridgman furnaces [7,12–15]. The crucibles were made of uncoated and graphite, boron nitride (BN), hexagonal BN, pyrolitic BN (pBN) coated fused silica. Contact angle of Ge on a pBN substrate has been measured up to 170° by Kaiser et al. [16]. Crystals grew partially or completely dewetted in the case of coated silica crucible.

Similarly, detached growth of InSb was obtained by Wilcox and Regel. They study the influence of two parameters: value of backfilling gas pressure and the nature of the inner wall coating. Best results were obtained for a backfilling pressure of 20 kPa Ar–10% H_2 and pBN-coated crucible. A model was given for detached solidification considering another source of gas pressure in the gap [17–19]. The excess of pressure in the cold gas phase is based on the release of dissolved gas at the solidification interface and its transport into the gap by diffusion and capillary convection.

In this work, the experiment configuration is designed by several critical parameters. Experiments are carried out on Earth and require the control of gas pressure difference to promote the dewetted growth. The crucible material and its preparation are kept identical for all experiments. Uncoated silica is the only material smooth enough in order to allow neglecting surface roughness effect on wetting. The transparency of silica allows observing the melt, the crystal and the solidification front. The backfilling pressure is kept constant. We study therefore the dewetting behaviour of two molten antimonides with a quasi-equal sum of the growth and contact angles: $132° \leq \theta + \alpha_{(InSb)} \leq 142°$ and $131° \leq \theta + \alpha_{(GaSb)} \leq 139°$. The objective is to perform dewetted growth successfully by observing in situ the two triple lines and the meniscus behaviour during the different steps of the sample growth in a low purity atmosphere.

2. Experimental procedure

2.1. Preparation of the feed material

For each experiment, the feed material is synthesized from high-purity elements by mean of an electromagnetic induction set-up. Gallium, indium and antimony are supplied by Wafer Technology. The purity grade is 6N. A description of the feed material preparation has been detailed by Mitric et al. [20]. To synthesize indium and gallium antimonide, indium and antimony blocks are cut into pieces of a few millimetres size. Indium chunks are etched by HNO_3-65% to remove oxide skins from

their surface, rinsed by deionised water and pure ethylic alcohol. Antimony pieces are immersed in a hydrochloric solution (HCl-35%). Cleaning is made with a burette by adding droplets of hydrogen peroxide H_2O_2-30% in the mixing of HCl-35% solution and Sb pieces. The experimenter should be cautious in this process as pouring H_2O_2 generates an exothermic reaction that is accompanied by the release of dichlorine gas Cl_2. Sb chunks are rinsed four times with HCl-35%, then with deionised water and pure ethylic alcohol.

The fused silica crucibles are of Herasil grade from Heraeus and supplied by Mondiaquartz that guarantees a rigorous cleaning of the delivered tubes by their original procedure. Crucible length with a flat bottom is 50 cm. The outer and inner diameters are respectively of 15 and 11 mm with ± 0.3 mm accuracy. They are packed in a specific polyethylene plastic in a class 100 clean room. The crucibles are systematically cleaned again in our laboratory after 10 weeks of storage. Before cleaning, the inner diameter is systematically measured with a Mitutoyo Holtest offering $\pm 2\,\mu$m measurement precision. Crucibles are etched by a solution of (40% HF + 10% H_2O_2 + 50% H_2O) and rinsed by deionised water and pure ethylic alcohol. The drying is made with a burner under dynamic high vacuum (5×10^{-5} mbar).

Ga and In are introduced and melted in the silica fused crucible. Liquid gallium or indium is degassed under dynamic vacuum at 5×10^{-5} mbar to remove dissolved gas and avoid the presence of gas bubbles. The vacuum system consists of a primary mechanic pump and secondary oil diffusion pump as secondary one. An accurate mass of Sb pieces is then introduced into the crucible in order to reach the stoichiometric composition with 10^{-2} mg accuracy. The crucible is sealed under dynamic vacuum at 5×10^{-5} mbar.

The feed material, that is the compound material, is synthesized with the use of an alternating magnetic field. This method favours the reaction of the compound formation by dynamically improving the mixing between the two pure elements [20].

The sample dedicated to the dewetting experiment is prepared from the feed material whose composition is close to the stoichiometry (determined quantitatively by WDX and micro-PIXE, see details in [20]). It must be emphasized that InSb is often difficult to remove from its synthesis silica crucible. Strong adhesion has been observed and leads sometimes to the break of the elaborated material due to sticking on the silica wall. On the contrary, GaSb is often easily removed from its silica crucible at this step. Sample length is 88 mm after cutting the elaborated material with a diamond saw. The outer surface of the sample is carefully polished with silicon carbide (1200, 2400 and 4000). The sample diameter is measured with a calliper whose precision measurement range is of $\pm 10\,\mu$m. The aim is to obtain a tight contact between the sample and the wall of the crucible especially at the level of the seed. Before insertion in a new cleaned silica crucible, the samples are cleaned with (50 ml HNO_3-65%, 50 ml HCl-37%) for 10 s, rinsed with pure HCl, then H_2O, then pure ethyl alcohol. The sample support is also made of the same fused silica and cleaned by the same procedure. The support length is 80 mm. The outer and inner diameters are 10 and 6 mm, respectively. Both support and sample are inserted into the crucible that is connected to the backfilling gas and vacuum system. The backfilling gas is standard argon provided by Air Products containing a few ppm of O_2 (>2 ppm). The crucible is sealed at 200 mbar with this argon. The height of the free volume above the sample is fixed to 5 cm by the sealing spot and is kept constant for each experiment. An illustration of a crucible-sample-support assembly is given in Fig. 2.

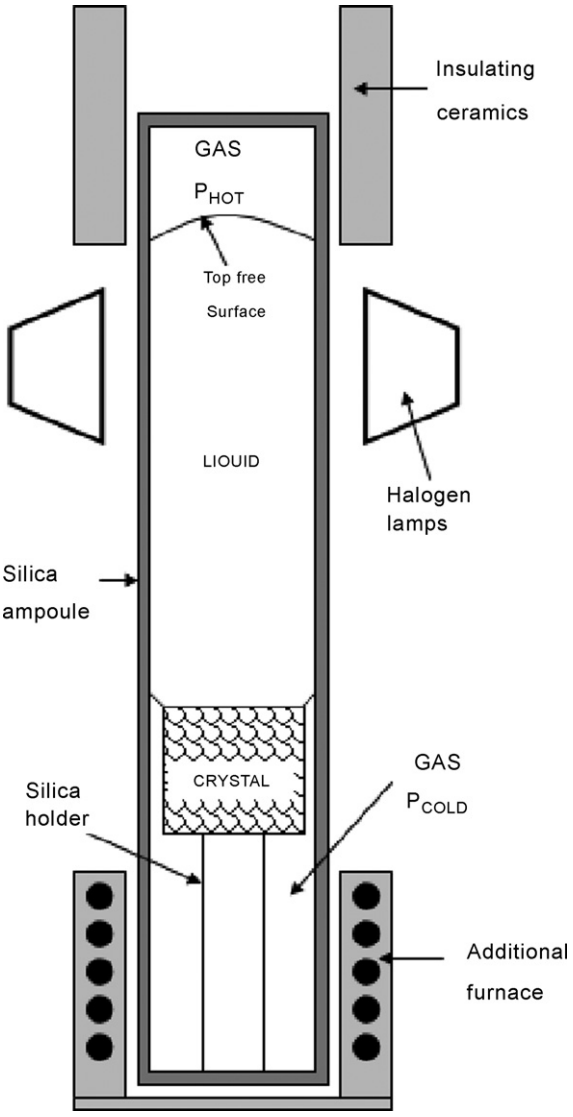

Fig. 2. Diagram of a sample–ampoule assembly for the dewetting experiment after melting and just before the solidification.

2.2. *Dewetting experimental set-up and procedure*

The experimental procedure consists of four steps: (1) melting a part of the feed material, (2) obtaining a meniscus at the liquid–non-molten solid junction (seeding procedure), (3) increasing the pressure in the cold part of the crucible in order to equilibrate the hydrostatic and hot pressures, and (4) pulling the furnace.

The set-up consists of a mirror furnace equipped with three identical tungsten halogen lamps provided by Osram (64635 HLX). The three lamps are inserted and fixed in a metallic

body made of aluminum alloy. Their maximum electric power is 150 W and 10 A maximum ac current. They are mounted in series to equalize the value of the alternating current passing through the three tungsten filaments. The semi-spherical reflectors of the lamps are covered by a thin gold layer to reflect effectively the rays intensity and thus the heat. The position of the bulbs ensures to focus the rays of light emitted from the filament on the crucible axis. The furnace body is fixed on two rods that are translated vertically thanks to the assembly of engines and speed variator. Accordingly, the melting and the solidification are respectively ensured by the downwards and upwards pulling of the furnace whereas the crucible is motionless. A dimmer switch equipped with a potentiometer supplied the engines with power and allows selecting manually the pulling rate from 5 to 50 mm h^{-1}. The maximum pulling distance from the lowest position of the furnace is 40 mm. The furnace has two windows to observe the bottom and top parts of the sample.

The additional furnace is made of a Ni/Cr heating wire provided by Thermocoax that is coiled on a drilled-metallic cylinder and covered by an insulating piece made of ceramics. Three holes are made within the cylinder to place the controller thermocouples and measure the longitudinal temperature homogeneity of the additional furnace. This furnace holds the silica crucible such as its symmetry axis passes through the gravity centre of the three bulbs. It is designed to increase the gas pressure in the cold part of the crucible by simply heating it.

The electric circuit was designed to control indirectly the position of the solidification front during an experiment and the temperature of the bottom furnace to increase the gas pressure on the bottom part of the crucible P_{COLD} according to the ideal gas law. A regulator of PID type (proportional, integral, derivative) marketed by Eurotherm controls two different voltages which are supplied to the bulbs and the bottom furnace. Hence, the electric circuit consists of two loops comprising the same devices: the dc output voltage of a regulator loop controls a thyristor wired up to the secondary of a voltage adaptor and to the resistive electric load (the bulbs or the furnace). Two ways are possible to control the solidification process and the gas pressure P_{COLD}:

(1) The controller operates in manual mode for the circuit comprising the lamps: the controlling parameter is the dc output voltage percentage of the controller. We performed a set of measurements to determine the maximum rate at which the bulbs reach their maximum power and saturate. The temperature increases in the crucible by increasing the output power manually. The solid/liquid interface is moved by the variation of the output power rate. When the interface is at the desired level, the value of the output voltage rate is fixed and the pulling starts.
(2) The controller operates in automatic mode for the circuit comprising the additional furnace: the controlling parameter is the temperature measured by a K-thermocouple located in the additional furnace body.

A set of temperature measurements was carried out with a dummy crucible to determine the temperature field within a dummy sample. The unsealed crucible contained an alumina tube of 88 mm length on an 80 mm fused silica support. Six thermocouples were inserted inside the alumina tube filled with alumina cement. The alumina tube and cement have the same thermal conductivity than InSb and GaSb at their melting temperature. The temperature drops rapidly from the ampoule height to the top and bottom parts of the dummy sample, giving rise to high values of the axial temperature gradient (up to 120 K cm^{-1}). This is the main drawback of the Bridgman mirror furnace. Hence, a thick white ceramic piece was added to thermally insulate the gas volume P_{HOT} (Fig. 3) and to reduce the heat loss in the hot part. The ampoule centring in the top extremity is also improved by this cylindrical piece. It has been concluded from theses measurements that both antimonides can be melted: $T_{melting}$ (InSb) = 798 K; $T_{melting}$ (GaSb) = 904 K. The height of the non-molten sample is 20 mm, the liquid height to melt is therefore of 68 mm. The maximum pulling distance from the lowest position of the furnace is 40 mm. The end of the solidification is performed by using the automatic mode. A negative ramp is applied on the output voltage rate so as to solidify at a velocity equal to that of pulling. This process is similar to the vertical gradient freeze (VGF).

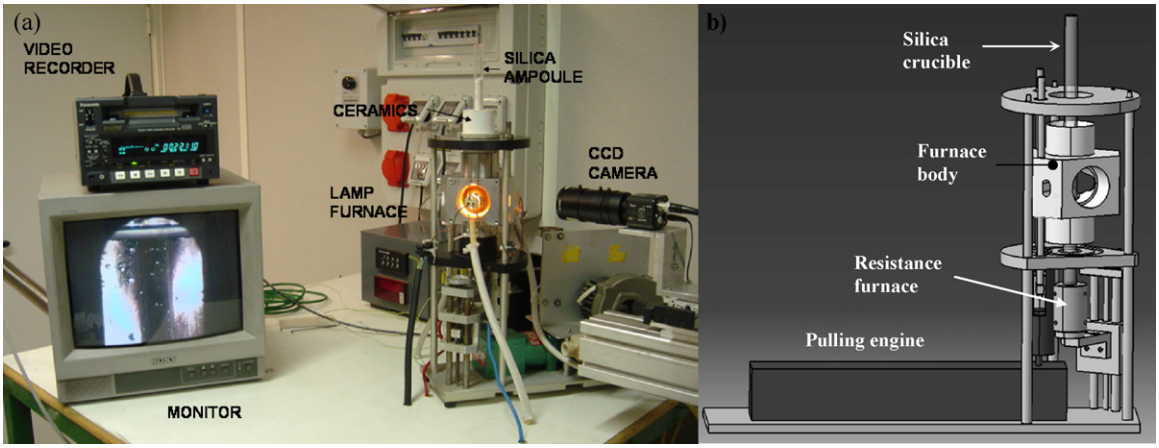

Fig. 3. (a) Picture of the dewetting experimental set-up. The image of a sample can be seen on the monitor before melting; (b) three-dimensional diagram of the body furnace, resistance furnace supporting the ampoule and the mechanic pulling system. The bulbs and the insulating ceramics are removed on purpose.

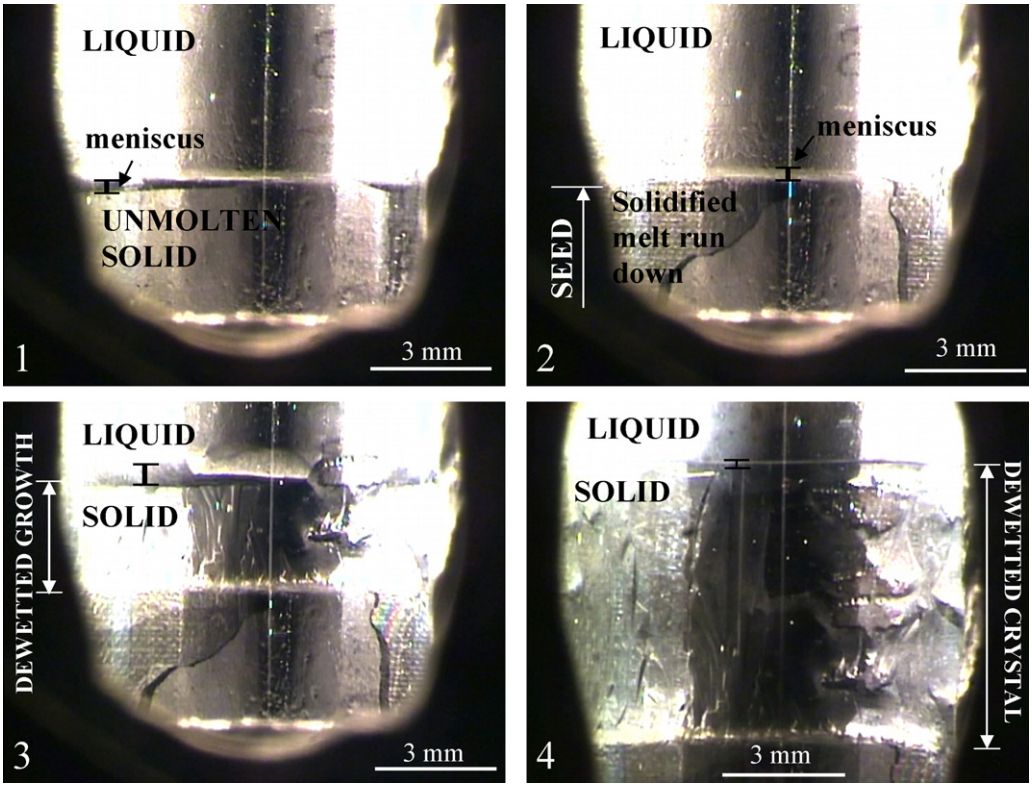

Fig. 4. Snapshots of the video recording of a GaSb dewetted growth. The camera displays the image visualized through the silica ampoule: (1) seeding step—the solid seed can be seen on the bottom separated from the above liquid by the liquid meniscus; (2) pulling starts—the looseness being wide in this experiment (>100 μm), melt run-down occurred at the beginning. The melt solidified as soon as it contacted the silica wall; (3) dewetted solidification—the solid/liquid interface went up without contact with the crucible wall. The surface morphology of the growing solid is typical of the free growth of the melt (facets and ridges); (4) idem, later.

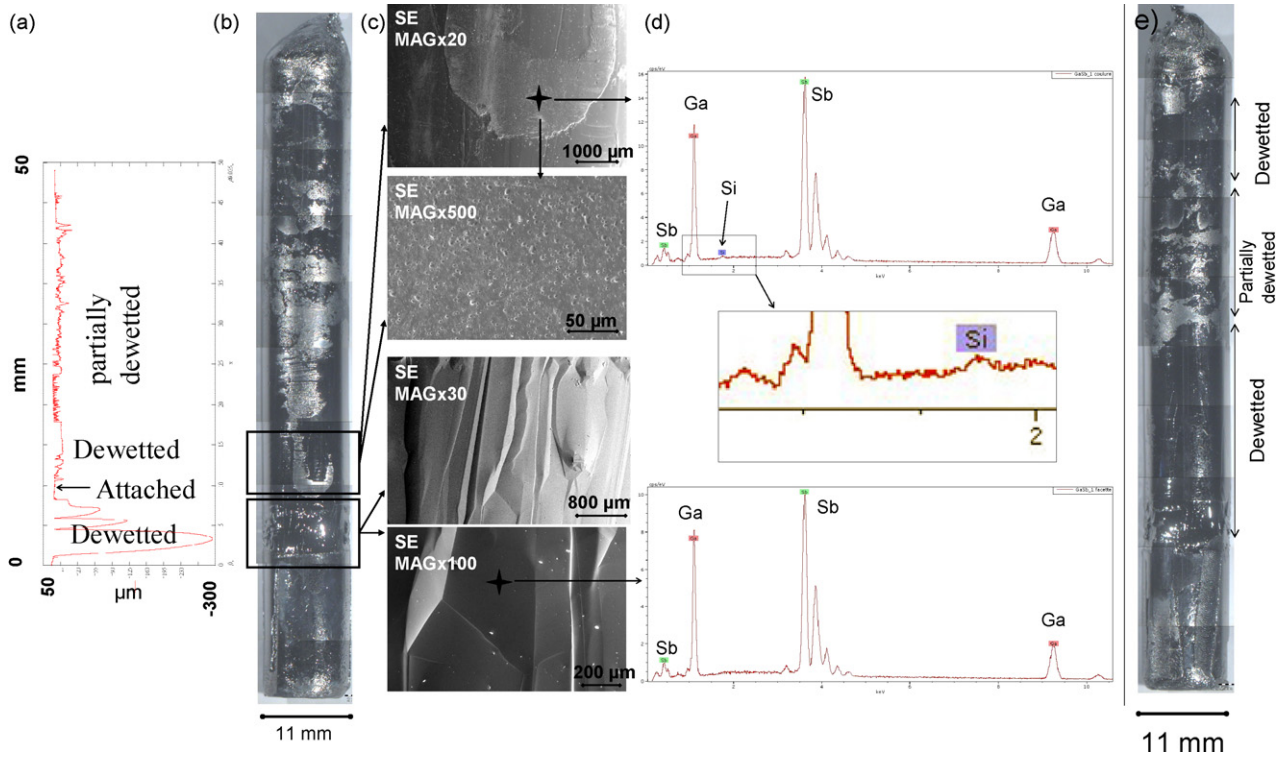

Fig. 5. From the left to the right: (a) surface profile of a dewetted GaSb polycrystal, (b) front view of the corresponding dewetted GaSb, (c) scanning electron microscopy: secondary electrons images at different magnitudes, (d) energy-dispersive X-ray spectra measured on the indicated spots, and (e) the second front view comes from the same sample but on a different face showing a different dewetted surface pattern.

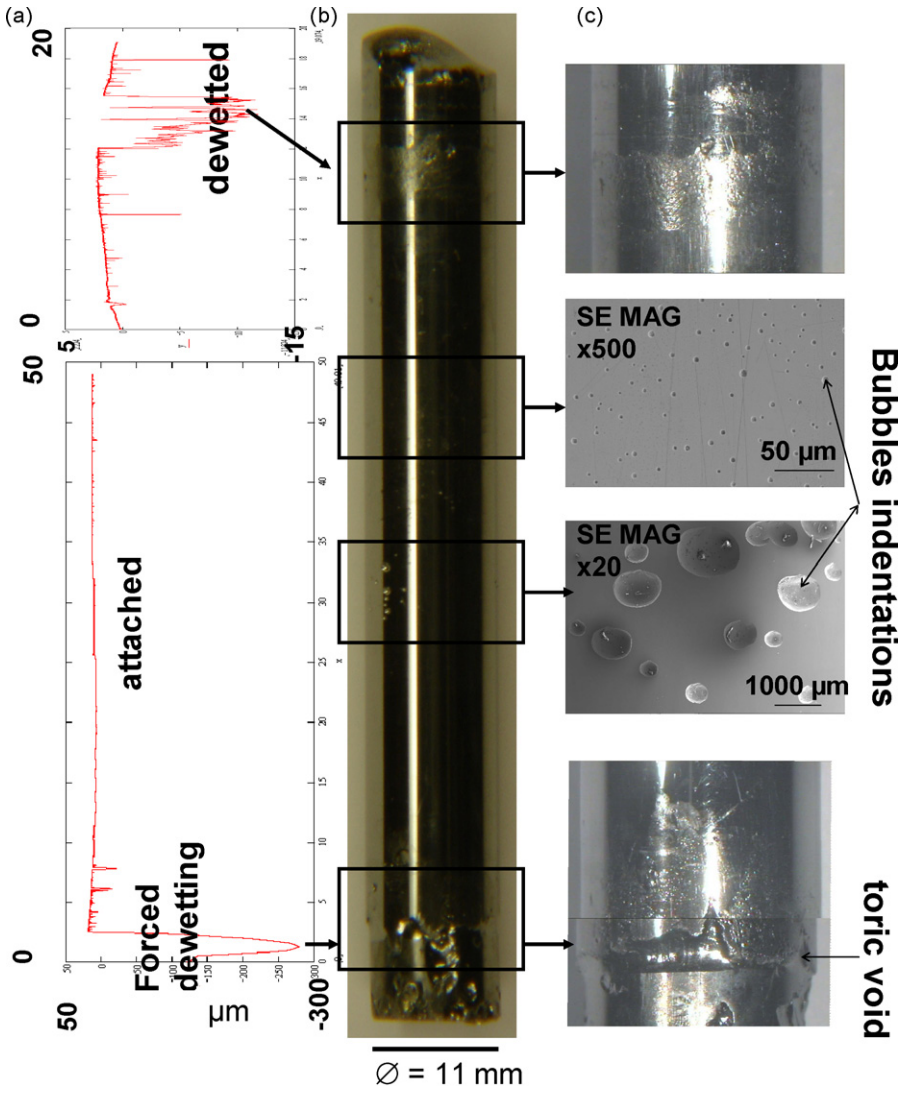

Fig. 6. (a) Surface profile, (b) front view, and (c) scanning electron micrographs of an attached InSb polycrystal. Observation of the toric void at the unmolten/resolidified level with $\Delta T_{COLD} = 10$ K. Dewetting occurred at the end with vanishing P_{HYD}.

The video recording is made with a Sony CCD camera connected to a monitor to visualize the solidification in real time and a DVC tape recorder.

3. Results and discussion

3.1. Recorded video sequences

The camera targets the bottom window of the body furnace and displays the image through the transparent silica crucible. We use the top window at the beginning of the procedure to visualize the top free surface and then perform the seeding procedure.

It is striking to observe the sensitivity of the solid/liquid interface position to any variation of the controller output voltage rate. The reproducibility of the values of the applied voltage is very satisfying for the seeding procedure. GaSb requires almost the maximum power to be melted on a 20 mm seed, circa 450 W, whereas InSb requires 250 W. We observed two different wetting behaviours between both molten antimonides at each step of the process. Each liquid meniscus is characterized by a horizontal band whose reflection of light is different from that of the liquid and the solid. The GaSb meniscus is bounded by two parallel and horizontal triple-lines. The InSb meniscus has a non-perfect horizontal ampoule-liquid–gas triple-line whereas the solid/liquid interface is planar. When P_{COLD} is increased, the InSb meniscus is much more sensitive to temperature variations and distorted. Bubbles formation can be seen when ΔT_{COLD} is equal to 10 K. As a result, we did not succeed to obtain dewetted growth of InSb even by forcing it at the seeding procedure. The transition between the seed and the beginning of the growth is always characterized by high values of gap thickness. This zone of the surface is referred as "forced dewetting" because it results from the increase of P_{COLD} which can produce a toric void followed by attached growth.

The GaSb meniscus is more stable for higher ΔT_{COLD} and keeps its two triple-lines parallel to each other on the recorded images as shown in Fig. 4. ΔT_{COLD} varied from 5 to 40 K dur-

ing the stable dewetted growth ($T_{\mathrm{COLD\,max}} = 358$ K). This result is surprising because the melt column above the seed is equal in the case of GaSb and InSb and thus P_{HYD} should be the same. Bubble formation was not observed but melt run-down occurred during the melting in the case of large looseness. Fig. 4 shows a GaSb dewetted growth sequence recorded by video. High growth velocities had no influence on the dewetting occurrence. The video sequence shown in Fig. 4 is recorded with a solid/liquid growth velocity of 100 mm h^{-1}. The pulling velocity is then reduced to 5 mm h^{-1}. The meniscus still existed at the level where the pulling velocity is modified and dewetted growth continued afterwards.

3.2. Analysis of ingot surfaces

Figs. 5 and 6 summarize the results of surface analysis. Surface profiles have been made with a profilometer. Fig. 5 shows the GaSb surface which is dewetted on 70% of its height. The first part is characterized by the presence of free melt growth morphologies such as facets where the gap thickness is up to 300 μm. The surface is shiny. Some areas are partially dewetted and contain ridges and islands corresponding to punctual attached zones. Stable dewetted growth is characterized by a narrow gap thickness of 15–20 μm along several centimetres on the GaSb surface. The end of the sample is mostly attached where the surface appears dull. Numerous bubbles indentations can be observed on attached spots. EDS analysis revealed qualitatively the presence of silicon in some surfaces in contact with the inner wall indicating a contamination by the silica ampoule. No bubbles are seen on dewetted areas and it was seen that the presence of a meniscus cause disappearance of any bubble after its crossing.

Fig. 6 illustrates the case of InSb which grew attached. The transition between the seed and the resolidified sample is characterized by a toric bubble formed by the forcing P_{COLD}. Contrarily to GaSb, attached surfaces of InSb are shiny whereas the small dewetted surface is rough and dull (P_{HYD} is vanishing at the end of the growth). Bubbles indentations are systematically visible on the attached surfaces at different magnitudes.

4. Conclusion

A dewetting phenomenon has been clearly identified and visualized compared to attached growth and confirmed by using complementary analysis: accurate measurement of surface profile with the profilometer, surface imaging with scanning electron microscopy, observation of bubbles indentations and contamination by silicon on attached areas detected by energy-dispersive X-ray spectrometry.

Dewetted growth has been successfully obtained for GaSb on uncoated fused silica with a low purity backfilling gas. On the contrary, attached growth occurs mainly in the case of InSb. Our experimental results show that both antimonides have not the same crucible/melt interaction under the same conditions during the growth experiments. This difference is surprising at first sight because these materials have comparable density, surface tension, growing and contact angles. It can be explained by the establishment of chemical interactions at the crucible/liquid interface or the role of dissolved oxygen in the melt affecting contact angles. The choice of a low purity Ar has been made to make a correlation with space experiments where dewetted growth of molten semiconductors occurred in open and smooth crucibles, i.e. without ΔP across the meniscus. The long storage of cartridges before launch could lead to outgassing of gaseous impurities. We are currently performing a new campaign of terrestrial experiments under high purity inert and reducing atmospheres and equilibrium thermodynamic calculation to determine the role of oxygen in these systems and on the dewetting phenomenon.

Acknowledgments

The authors acknowledge the financial support by the European Space Agency (ESA) under contract MAP-99-035 and by the French space agency (CNES). The authors are grateful to Dr. Francine Roussel-Dherbey from CMTC (INPG-France) for the helpful assistance in SEM imaging and EDS analysis.

References

[1] T. Duffar, P. Boiton, P. Dusserre, J. Abadie, J. Crystal Growth 179 (1997) 397.
[2] W.R. Wilcox, L.L. Regel, Microgravity Sci. Technol. VIII (1) (1995) 56.
[3] W.R. Wilcox, L.L. Regel, Microgravity Sci. Technol. XI (4) (1998) 152.
[4] T. Duffar, I. Harter, P. Dusserre, J. Crystal Growth 100 (1990) 171.
[5] T. Duffar, P. Dusserre, N. Giacometti, J. Crystal Growth 223 (2001) 69.
[6] T. Duffar, P. Dusserre, F. Picca, S. Lacroix, N. Giacometti, J. Crystal Growth 211 (2000) 434.
[7] W. Palosz, M.P. Volz, S. Cobb, S. Motakef, F.R. Szofran, J. Crystal Growth 277 (2005) 124.
[8] T. Duffar, J. Abadie, Int. J. Microgravity Sci. Technol. IX (1) (1996) 35.
[9] E. Balikci, A. Deal, R. Abbashian, J. Crystal Growth 262 (2004) 581.
[10] I. Harter, P. Dusserre, T. Duffar, J.-P. Nabot, N. Eustathopoulos, J. Crystal Growth 131 (1993) 157.
[11] A.K. Kota, G. Anand, S. Ramakrishnan, L.L. Regel, W.R. Wilcox, J. Crystal Growth 290 (2006) 319.
[12] P. Dold, F.R. Szofran, K.W. Benz, J. Crystal Growth 234 (2002) 91.
[13] M.P. Volz, M. Schweizer, N. Kaiser, S.D. Cobb, L. Vujisic, S. Motakef, F.R. Szofran, J. Crystal Growth 237–239 (2002) 1844.
[14] M. Schweizer, M.P. Volz, S.D. Cobb, L. Vujisic, S. Motakef, J. Szoke, F.R. Szofran, J. Crystal Growth 237–239 (2002) 2107.
[15] O. Pätzold, K. Jenkner, S. Scholz, A. Cröll, J. Crystal Growth 277 (2005) 37.
[16] N. Kaiser, A. Cröll, F.R. Szofran, S.D. Cobb, K.W. Benz, J. Crystal Growth 231 (2001) 448.
[17] D.I. Popov, L.L. Regel, W.R. Wilcox, J. Mater. Synth. Proc. 5 (1997) 283.
[18] D.I. Popov, L.L. Regel, W.R. Wilcox, J. Mater. Synth. Proc. 5 (1997) 299.
[19] D.I. Popov, L.L. Regel, W.R. Wilcox, J. Mater. Synth. Proc. 5 (1997) 313.
[20] A. Mitric, V. Corregidor, L.C. Alves, A. Amariei, C. Diaz-Guerra, J. Piqueras, J. Crystal Growth 275 (2005) e601.